

## Percolation framework to describe El Niño conditions

Jun Meng,<sup>1,2</sup> Jingfang Fan,<sup>1,a)</sup> Yosef Ashkenazy,<sup>2</sup> and Shlomo Havlin<sup>1,3</sup>

<sup>1</sup>Department of Physics, Bar Ilan University, Ramat Gan 52900, Israel

<sup>2</sup>Solar Energy and Environmental Physics, Blaustein Institutes for Desert Research, Ben-Gurion University of the Negev, Beersheba, 84996, Israel

<sup>3</sup>Institute of Innovative Research, Tokyo Institute of Technology, 4259 Nagatsuta-cho, Midori-ku, Yokohama 226-8502, Japan

(Received 15 November 2016; accepted 25 January 2017; published online 22 February 2017)

Complex networks have been used intensively to investigate the flow and dynamics of many natural systems including the climate system. Here, we develop a percolation based measure, the order parameter, to study and quantify climate networks. We find that abrupt transitions of the order parameter usually occur  $\sim 1$  year before El Niño events, suggesting that they can be used as early warning precursors of El Niño. Using this method, we analyze several reanalysis datasets and show the potential for good forecasting of El Niño. The percolation based order parameter exhibits discontinuous features, indicating a possible relation to the first order phase transition mechanism.

Published by AIP Publishing. [<http://dx.doi.org/10.1063/1.4975766>]

**Climate conditions influence the nature of societies and economies. El Niño event, in particular, has great influences on climate, which may further cause widespread natural disasters like flood and drought across the globe. We have just undergone one of the strongest El Niño events (2014–2016) since 1948, it brings drought conditions in Venezuela, Australia, and more tropical cyclones within the Pacific Ocean. There have been still improvements in the understanding of El Niño, its climate effects and associated impacts. Here, we present a multidisciplinary renaissance combined climate, network, and percolation theory to study the mechanism of El Niño. Our method can forecast El Niño events 1 year-ahead of the events, with a high prediction accuracy of 70%, and a low false alarm of only 4%. The methodology and results presented here not only facilitate the study of predicting El Niño events but also can bring a fresh perspective to the study of abrupt phase transitions.**

### I. INTRODUCTION

In the last two decades, complex network became a popular framework to investigate a large variety of real systems, including Internet, social networks, biological networks, and financial networks.<sup>1–5</sup> In recent years, network approach was found to be useful in studying climate phenomena, using “climate network.”<sup>6–18</sup> In a climate network, usually, nodes are chosen to be geographic locations, and links are constructed based on the similarities between the time variability between pairs of nodes. Climate networks are used to quantify and analyze the structure and dynamics of the climate system<sup>19–23</sup> and even forecast some important climate phenomena, such as monsoon,<sup>24–26</sup> the North Atlantic Oscillation,<sup>27,28</sup> and El Niño.<sup>8,15,16,19,29,30</sup>

El Niño is probably the most influential climate phenomenon on interannual time scales.<sup>31–34</sup> During El Niño,

the eastern Pacific Ocean is getting warmer by several degrees, impacting the local and global climate. La Niña is cold anomaly over the El Niño region. The El Niño activity is quantified, for example, by the Oceanic Niño Index (ONI), which is NOAA’s primary indicator for monitoring El Niño and La Niña. El Niño can trigger many disruptions around the globe and in this way affect various aspects of human life. These include unusual weather conditions, droughts, floods, declines in fisheries, famine, plagues, political and social unrest, and economic changes. Global impacts of El Niño had been investigated by Halpert and Ropelewski.<sup>35</sup> Here we propose a percolation framework analysis to describe the structure of the global climate system during El Niño, based on climate networks. Our results suggest that an abrupt first order percolation transition occur about 1 year ahead of El Niño events.

Percolation theory is also used to analyze the behavior of connected clusters in a network.<sup>5,36,37</sup> The applications of percolation theory cover many areas, such as, optimal path, directed polymers, epidemics, immunization, oil recovery, and nanomagnets. In the framework of percolation theory, one may define phase transition based on simplest pure geometrical considerations.

In the present study, we construct a sequence of monthly shifting-climate networks by adding links one by one according to the similarities between nodes. More specifically, the nodes which are more similar (based on their temperature variations) will be connected first. We statistically found that around one year prior to the onset of El Niño, the climate network undergoes a first order phase transition (i.e., exhibiting a significant discontinuity in the order parameter), indicating that links with higher similarities tend to localize into two large clusters, in the higher latitudes of the northern and southern hemispheres. However, during El Niño event periods, there is only one big cluster via tropical links. We find that indications of discontinuity in the order parameter are closely related to the ONI.

<sup>a)</sup>Electronic mail: j.fang.fan@gmail.com

## II. CLIMATE NETWORK

Our analysis is based on the daily near surface (1000 hPa) air temperature of ERA-Interim reanalysis.<sup>38</sup> We pick 726 grid points that approximately homogeneously cover the entire globe;<sup>19</sup> these grid points are chosen to be the nodes of our climate network. For each node (i.e., longitude-latitude grid point), daily values within the period 1979–2016 are used, from which we subtract the mean seasonal cycle and divide by the seasonal standard deviation. Specifically, given a record  $\tilde{T}^y(d)$ , where  $y$  is the year, and  $d$

stands for the day (from 1 to 365), the filtered record is defined as

$$T^y(d) = \frac{\tilde{T}^y(d) - \text{mean}(\tilde{T}(d))}{\text{std}(\tilde{T}(d))}, \quad (1)$$

where “mean” and “std” are the mean and standard deviation of the temperature on day  $d$  over all years.

To obtain the time evolution of the strengths of the links between each pair of nodes, we define, the time-delayed cross-correlation function as

$$C_{ij}(-\tau) = \frac{\langle T_i(d)T_j(d-\tau) \rangle - \langle T_i(d) \rangle \langle T_j(d-\tau) \rangle}{\sqrt{(\langle T_i(d) \rangle - \langle T_i(d) \rangle)^2} \cdot \sqrt{(\langle T_j(d-\tau) \rangle - \langle T_j(d-\tau) \rangle)^2}}, \quad (2)$$

and

$$C_{ij}(\tau) = \frac{\langle T_i(d-\tau)T_j(d) \rangle - \langle T_i(d-\tau) \rangle \langle T_j(d) \rangle}{\sqrt{(\langle T_i(d-\tau) \rangle - \langle T_i(d-\tau) \rangle)^2} \cdot \sqrt{(\langle T_j(d) \rangle - \langle T_j(d) \rangle)^2}}, \quad (3)$$

where  $\tau$  is the time lag between 0 and 200 days. Note that for estimating the cross-correlation function at day  $d$ , only the temperature data points prior to this day are considered. We then define the link’s weight as the maximum of the cross-correlation function  $\max(C_{ij}(\tau))$ .

## III. PERCOLATION

In lattices model, a percolation phase transition occurs if the systems’ dimension is larger than one.<sup>37</sup> The system is considered percolating if there is a path from one side of the lattice to the other, passing through occupied bonds (bond percolation) or sites (site percolation). The percolation threshold usually depends on the type and dimensionality of the lattice. However, for the network system, no notion of side exists. For this reason, a judgment condition to verify whether the system is percolating is the existence of a giant component (cluster) containing  $O(N)$  nodes, where  $N$  is the total number of nodes in the network. If two nodes are in the same cluster, then there is at least one path passing through them.

In this section, we discuss the construction of the climate networks, and study the evolution of clusters. Initially, given  $N=726$  isolate nodes, links are added one by one according to the link strength, i.e., we first add the link with the highest weight, and continue selecting edges ordered by decreasing weight. During the evolution of our network, we measure the size of the normalized largest cluster  $s_1 = S_1/N$  and the susceptibility  $\chi$ , where  $S_1$  represents the size of the largest component. The size of the largest cluster is defined as the number of nodes in the largest component.<sup>5</sup> A component is a subset of nodes of a network such that there exists at least one path from each node in that subset to another

node in the subset.<sup>4</sup> The susceptibility of the climate network (the average size of the finite clusters) is defined as<sup>36</sup>

$$\chi = \frac{\sum'_s s^2 n_s(C)}{\sum'_s s n_s(C)}, \quad (4)$$

where  $n_s(C)$  denotes the average number of clusters of size  $s$  at edge’s weight  $C$ , and the prime on the sums indicates the exclusion of the largest cluster in each measurement.

Since our network is finite, we use the following procedure to find the percolation threshold. We first calculate, during the growth process, the largest size change of the largest cluster:

$$\Delta \equiv \frac{1}{N} \max[S_1(C_2) - S_1(C_1), \dots, S_1(C_{T+1}) - S_1(C_T), \dots], \quad (5)$$

where  $C_T$  are the links’ weights ordered by decreasing value. The step with the largest jump is defined as  $C_c$ . The percolation transition in the network is characterized by  $\Delta$ , and  $C_c$  corresponds to its transition point. We find that the magnitude of  $\Delta$  has a strong correlation with El Niño Index (see Fig. 1), but the susceptibility has seemingly no distinct relation with El Niño Index. We thus refrain from using the susceptibility as a predictor of El Niño but only use it to validate the “location” of the percolation transition.

## IV. RESULTS

For each network, we obtain  $\Delta$ , and find that, usually around one year ahead of the beginning of El Niño, the climate network has the largest  $\Delta$ . This feature is used here for forecasting the inception of an El Niño event in the

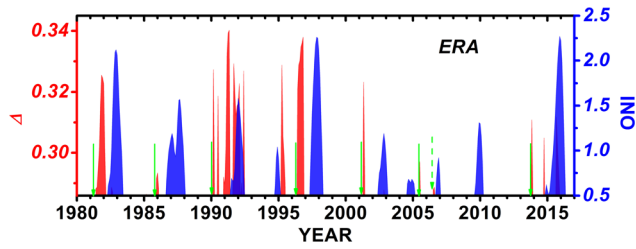


FIG. 1. The percolation forecasting scheme and power based on the near surface temperature of the ERA-Interim dataset.<sup>38</sup> We compare the largest gap of the largest cluster  $\Delta$  during the climate network evolution with a threshold  $\Theta = 0.286$  (red curve, left scale) and the ONI (blue curve, right scale) between January 1980 and September 2016. When the  $\Delta$  is above the threshold,  $\Theta$ , we give an alarm and predict that an El Niño event will start in the following calendar year. Correct predictions are marked by green arrows and false alarms by dashed arrows.

following year. To this end, we place a varying horizontal threshold  $\Delta = \Theta$  and mark an alarm when  $\Delta$  is above threshold, outside an El Niño episode. Fig. 1 demonstrates the forecasting power where the red curve depicts  $\Delta$ , and the blue curve is the ONI; correct predictions are marked by green arrows. The lead time between the prediction and the beginning of the El Niño episodes is  $1.05 \pm 0.18$  year. Our method forecasts 7 out of 10 events. Note the similarity in the power of forecasting to that of Ludescher *et al.*<sup>16</sup>

Next, we concentrate on specific El Niño events to illustrate the evolving cluster structure through El Niño. We first focus on one of the strongest El Niño events, the 1982–1983 event. In Fig. 2, we show for this event,  $s_1$  and  $\chi$  as a function of link strength  $C$  two years and one year before El Niño, during El Niño and one year after El Niño. We find that  $s_1$  exhibits the largest jump in  $\Delta$  about one year before El Niño; the jump in  $\chi$  also becomes very large at the same point. The two quantities yield the same percolation threshold, strengthening the confidence of the threshold value.

Fig. 3(a) shows the climate network cluster structure in the globe map at the percolation threshold one year before El Niño event. It seems like the equatorial region separates the

network into two communities, Northern and Southern hemispheres, where the nodes with green color indicate the largest cluster and the blue indicates the second largest cluster; after the critical link adding (marked by thicker green line), the largest and second largest cluster merge, and the new largest clusters approximately covers the entire globe (Fig. 3(b)). We find that typically during the El Niño event, (Fig. 2(c))  $s_1$  does not exhibit a large jump at the percolation threshold. Fig. 3(c) shows the cluster structure at the percolation threshold before the critical link was added. Fig. 3(d) shows the cluster structure at the percolation threshold, just after the critical link was added. There are more edges in the tropical zone. This is since during the El Niño period, the nodes in low latitudes are drastically affected by the El Niño, resulting in higher cross-correlation. Therefore, we do not find a large gap in the percolation of the network.

Another example for the evolution of the network (represented by  $s_1$  and  $\chi$  vs.  $C$ ) during the 1997–1998 El Niño event is shown in Fig. 4. Also here we find that one year before event there is a large gap in  $s_1$  (Fig. 4(b)), however, during the El Niño event, two years before the event and one year after the event, the gap becomes smaller (Figs. 4(a), 4(c), and 4(d)).

Following the above, we assume that large  $\Delta$  is an alarm forecast that El Niño will develop in the following calendar year. In the case of multiple alarms in the same calendar year, only the first one is considered. The alarm results in a correct prediction, if in the following calendar year, an El Niño episode actually occurs; otherwise it is regarded as a false alarm. There were 10 El Niño events (years) between 1980 and 2016 and additional 27 non-El Niño years. To quantify the accuracy of our prediction, we use the Receiver Operating Characteristic (ROC)-type analysis<sup>15</sup> when altering the magnitude of the threshold and hence the hit and false-alarm rates. Fig. 5 shows the best hit rates for the false-alarm rates 0, 1/27, 2/27, and 3/27. The best performances are for (i) thresholds  $\Theta$  in the interval between 0.286 and

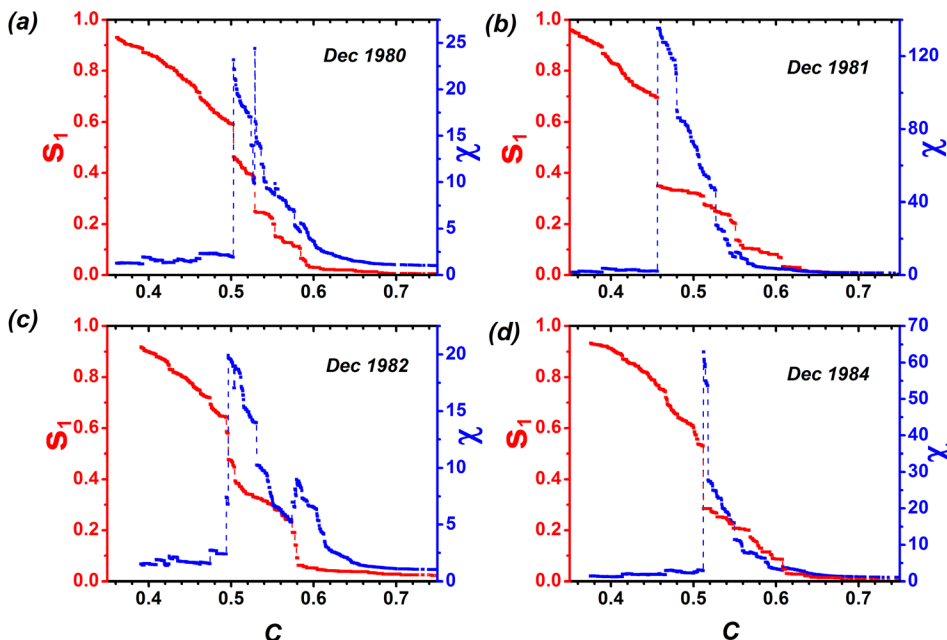


FIG. 2. The largest cluster  $s_1$  (red curve, left scale) and the susceptibility  $\chi$  (blue curve, right scale) as a function of the link strength  $C$ . (a) For the network two years before El Niño episode, where the end time is December 1980; (b) for the network one year before El Niño episode, where the end time is December 1981; (c) for the network during El Niño episode, where the end time is December 1982; (d) for the network one year after El Niño episode, where the end time is December 1984. Note the largest jump in  $\Delta$  one year prior to El Niño event.

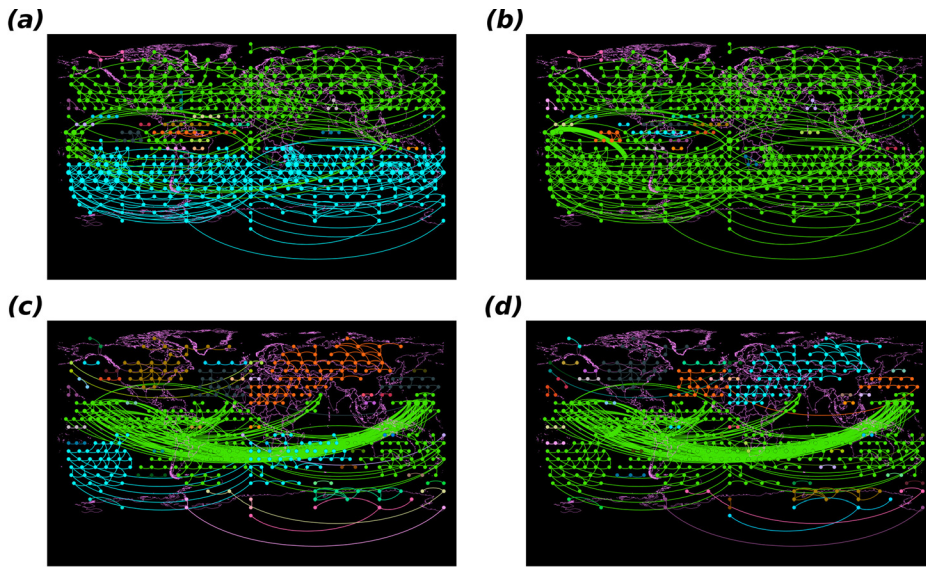


FIG. 3. The cluster structure on map at the percolation threshold for the network one year before the El Niño event (December 1981). (a) Before the critical link was added; (b) after the critical link (marked by thicker green line) was added. During El Niño episode (December 1982) (c) before the critical link was added and (d) after the critical link. Different colors represent different clusters, especially, the green represents the largest cluster and the blue represents the second largest cluster.

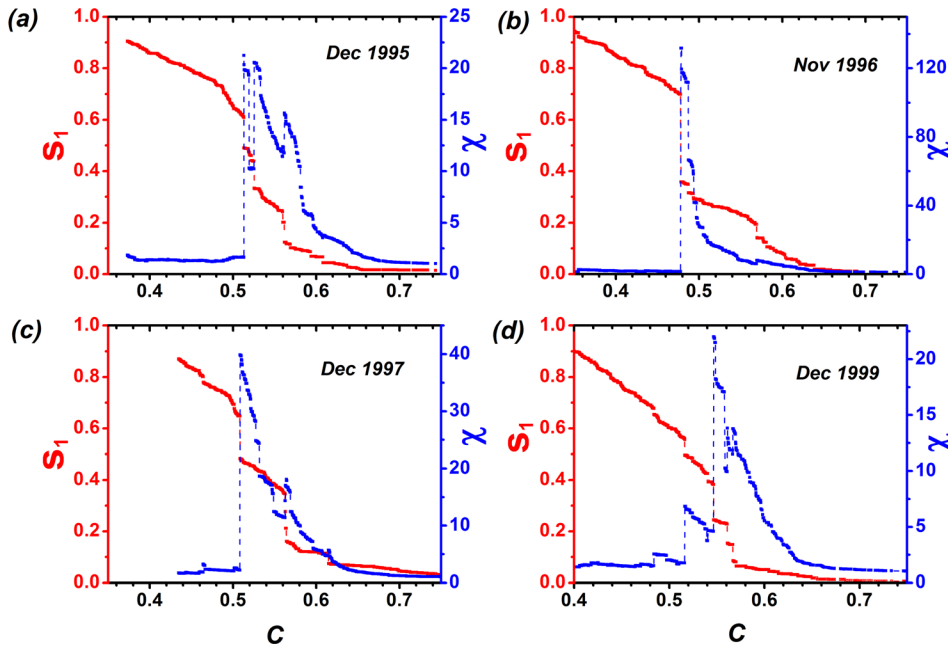


FIG. 4. Same as Fig. 2 for the strong 1997–1998 El Niño event.

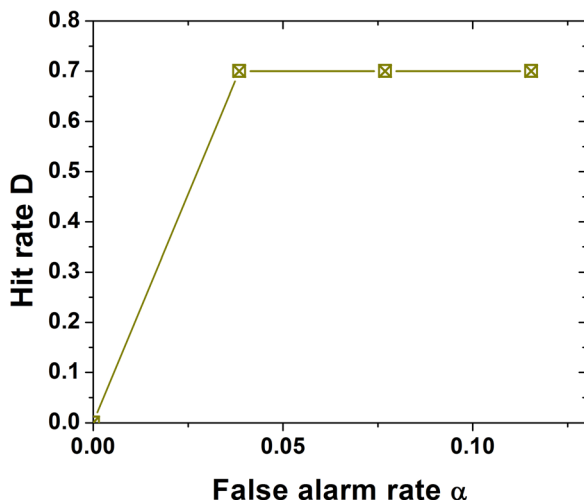


FIG. 5. The prediction accuracy of our method. For the four lowest false-alarm rates  $\alpha = 0, 1/27, 2/27, 3/27$  the best hit rates  $D$ .

0.289, where the false-alarm rate is  $1/27$  and the hit rate is  $0.7$ , for (ii) thresholds between  $0.264$  and  $0.266$ , where the false-alarm rate is  $2/20$  and the hit rate is  $0.7$ , and (iii) for thresholds between  $0.223$  and  $0.26$ , where the false-alarm rate is  $3/20$  and the hit rate is  $0.7$ .

We also applied the same method for different datasets, the NCEP/NCAR reanalysis dataset,<sup>39</sup> and the JRA-55 dataset.<sup>40</sup> The prediction accuracy is summarized in Table I. We basically find very similar results for all three different

TABLE I. The forecast accuracy for different reanalysis datasets, based on the Receiver Operating Characteristic (ROC)-type.

Dataset	Hit rates $D$	False-alarm rates $\alpha$
ERA-Interim (1980–2016)	7/10	1/27
NCEP/NCAR reanalysis (1980–2016)	6/10	1/27
JRA-55 (1980–2016)	6/10	1/27
NCEP/NCAR reanalysis (1950–2016)	14/22	4/47

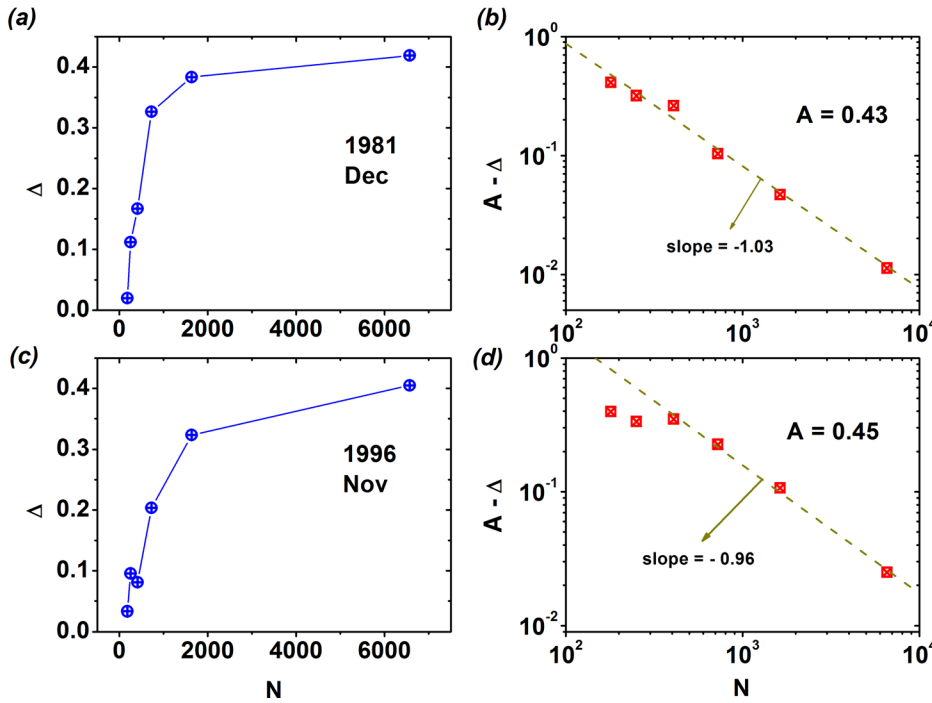


FIG. 6. The finite size effects for the networks before El Niño episode. The largest gap  $\Delta(N)$  as a function of system size  $N$  for (a) December 1981 and (b) November 1996. (b) and (d) Log-log plot of  $A - \Delta(N)$  versus  $N$ , indicating a possible scaling law with the scaling exponent  $\sim 1$ ; see Eq. (6).

reanalysis datasets, strengthening the confidence in our prediction method.

To further test the order of the percolation phase transitions in the climate network before El Niño event, we study the finite size effects of our network, and suggest that the transition is a first order phase transition. We change the system's size by altering the resolution of nodes, and at the same time make sure that every node in a given covers the same area on the global (i.e., we are fewer nodes at the high latitudes). First, we define the resolution (in degree latitude) at the Equator as  $r_0$  and then find that the number of nodes is  $n_0 = 360/r_0$ . Then the number of nodes in latitude  $r_0 m$  is  $n_m = n_0 \cos(r_0 m)$ , where  $m \in [-90/r_0, 90/r_0]$ . The total number of nodes is then  $N = \sum_{m=0}^{90/r_0} 2n_m - n_0$ . We choose  $r_0$  to be  $(15, 12.5, 10, 7.5, 5, 2.5)^\circ$ , which yields  $N = (180, 251, 408, 726, 1634, 6570)$ . We then calculate  $\Delta$  as a function of the system size  $N$ . If  $\Delta$  approaches zero as  $N \rightarrow \infty$ , the corresponding giant component is assumed to undergo a continuous percolation; otherwise, the corresponding percolation is assumed to be discontinuous. This is since it suggests that the order parameter  $s_1$  has a non-zero discontinuous jump at the percolation threshold.<sup>41,42</sup> The results of  $\Delta$  as a function of the system size  $N$  are shown in Fig. 6 for two El Niño events considered above. The results suggest a discontinuous percolation since  $\Delta(N)$  tends to be a non-zero constant (Figs. 6(a) and 6(c)). We also find that  $\Delta$  follows a scaling form:

$$A - \Delta(N) \sim N^{-\beta}, \quad (6)$$

where  $A$  is a constant and  $\beta$  is a critical exponent. Figs. 6(b) and 6(d) show the related results where we find that  $\beta$  is very close to 1, implying it might be an universal scaling exponent.

It has been pointed out that a random network always undergoes a continuous percolation phase transition during a

random process.<sup>43</sup> The question whether percolation transitions could be discontinuous have attracted much attention.<sup>44</sup> Discontinuous percolation in networks was reported in the framework of the explosive percolation model.<sup>45</sup> However, later studies questioned this finding.<sup>46–53</sup> Interestingly, our results indicate the possibility of first order phase transition in climate networks.

Recently, a percolation approach was used to study earth science<sup>54</sup> and climate systems.<sup>55</sup> Rodriguez-Mendez *et al.*<sup>55</sup> found precursors for both model simulations and climate phenomena (such as El Niño) based on percolation theory in functional networks; we find their results to be consistent with our conclusions, i.e., that abrupt transitions of the order parameter usually occur before El Niño. The advantage of the results and methods presented here is that the prediction time is about 1 year prior to El Niño.

## V. CONCLUSIONS

To summarize, a time-evolving weighted climate network is constructed based on the near surface air temperature time series. A percolation framework to study the cluster structure properties of the climate network is put forward. We find that the structure of the network changes violently approximately one year ahead of El Niño events—we suggest to use such percolation-based precursor, the largest change of order parameter,  $\Delta$ , to forecast El Niño events. The percolation description of climate system (as reflected by the surface air temperature records) highlight the importance of such network techniques to understand and forecast El Niño events. Based on finite size scaling analysis, we also find that the percolation process is discontinuous. The methodology and results presented here not only facilitate the study of predicting El Niño events but also can bring a fresh perspective to the study of abrupt phase transitions.

## ACKNOWLEDGMENTS

J. Fan thanks the fellowship program funded by the Planning and Budgeting Committee of the Council for Higher Education of Israel. We acknowledge the MULTIPLEX (No. 317532) EU project, the Italy-Israel NECST project, Japan-Israel scientific cooperation supported by MOST, the Israel Science Foundation, ONR and DTRA for financial support.

- <sup>1</sup>D. Watts and S. Strogatz, *Nature* **393**, 440–442 (1998).
- <sup>2</sup>A. Barabási and R. Albert, *Science* **286**, 509–512 (1999).
- <sup>3</sup>R. Albert and A. Barabási, *Rev. Mod. Phys.* **74**, 47–97 (2002).
- <sup>4</sup>M. Newman, *Networks: An Introduction* (Oxford University Press, 2010).
- <sup>5</sup>R. Cohen and S. Havlin, *Complex Networks: Structure, Robustness and Function* (Cambridge University Press, 2010).
- <sup>6</sup>A. A. Tsonis, K. L. Swanson, and P. J. Roebber, *Bull. Am. Meteorol. Soc.* **87**, 585 (2006).
- <sup>7</sup>A. A. Tsonis, K. L. Swanson, and S. Kravtsov, *Geophys. Res. Lett.* **34**, L13705, doi:10.1029/2007GL030288 (2007).
- <sup>8</sup>K. Yamasaki, A. Gozolchiani, and S. Havlin, *Phys. Rev. Lett.* **100**, 228501 (2008).
- <sup>9</sup>J. F. Donges, Y. Zou, N. Marwan, and J. Kurths, *Eur. Phys. J.: Spec. Top.* **174**, 157 (2009).
- <sup>10</sup>J. F. Donges, Y. Zou, N. Marwan, and J. Kurths, *Europhys. Lett.* **87**, 48007 (2009).
- <sup>11</sup>K. Steinhaeuser, N. V. Chawla, and A. R. Ganguly, *SIGKDD Explor.* **12**, 25 (2010).
- <sup>12</sup>K. Steinhaeuser, N. V. Chawla, and A. R. Ganguly, *Statist. Anal. Data Min.* **4**, 497 (2011).
- <sup>13</sup>M. Barreiro, A. C. Marti, and C. Masoller, *Chaos* **21**, 013101 (2011).
- <sup>14</sup>J. Deza, M. Barreiro, and C. Masoller, *Eur. Phys. J.: Spec. Top.* **222**, 511 (2013).
- <sup>15</sup>J. Ludescher, A. Gozolchiani, M. I. Bogachev, A. Bunde, S. Havlin, and H. J. Schellnhuber, *Proc. Natl. Acad. Sci. U.S.A.* **110**, 11742 (2013).
- <sup>16</sup>J. Ludescher, A. Gozolchiani, M. I. Bogachev, A. Bunde, S. Havlin, and H. J. Schellnhuber, *Proc. Natl. Acad. Sci. U.S.A.* **111**, 2064 (2014).
- <sup>17</sup>D. C. Zemp, M. Wiedermann, J. Kurths, A. Rammig, and J. F. Donges, *Europhys. Lett.* **107**, 58005 (2014).
- <sup>18</sup>J. Fan, J. Meng, X. Chen, Y. Ashkenazy, and S. Havlin, *Sci. China: Phys., Mech. Astron.* **60**, 010531 (2017).
- <sup>19</sup>A. Gozolchiani, S. Havlin, and K. Yamasaki, *Phys. Rev. Lett.* **107**, 148501 (2011).
- <sup>20</sup>J. F. Donges, H. C. H. Schultz, N. Marwan, Y. Zou, and J. Kurths, *Eur. Phys. J. B* **84**, 635 (2011).
- <sup>21</sup>K. Steinhaeuser, A. R. Ganguly, and N. V. Chawla, *Clim. Dyn.* **39**, 889 (2012).
- <sup>22</sup>Y. Wang, A. Gozolchiani, Y. Ashkenazy, Y. Berezin, O. Guez, and S. Havlin, *Phys. Rev. Lett.* **111**, 138501 (2013).
- <sup>23</sup>D. Zhou, A. Gozolchiani, Y. Ashkenazy, and S. Havlin, *Phys. Rev. Lett.* **115**, 268501 (2015).
- <sup>24</sup>N. Malik, B. Bookhagen, N. Marwan, and J. Kurths, *Clim. Dyn.* **39**, 971–987 (2012).
- <sup>25</sup>N. Boers, B. Bookhagen, N. Marwan, J. Kurths, and J. Marengo, *Geophys. Res. Lett.* **40**, 4386–4392, doi:10.1002/grl.50681 (2013).
- <sup>26</sup>N. Boers, B. Bookhagen, H. Barbosa, N. Marwan, J. Kurths, and J. Marengo, *Nat. Commun.* **5**, 5199 (2014).
- <sup>27</sup>O. Guez, A. Gozolchiani, Y. Berezin, S. Brenner, and S. Havlin, *Europhys. Lett.* **98**, 38006 (2012).
- <sup>28</sup>O. Guez, A. Gozolchiani, Y. Berezin, Y. Wang, and S. Havlin, *Europhys. Lett.* **103**, 68006 (2013).
- <sup>29</sup>A. A. Tsonis and K. L. Swanson, *Phys. Rev. Lett.* **100**, 228502 (2008).
- <sup>30</sup>A. Radebach, R. V. Donner, J. Runge, J. F. Donges, and J. Kurths, *Phys. Rev. E* **88**, 052807 (2013).
- <sup>31</sup>H. Dijkstra, *Nonlinear Physical Oceanography: A Dynamical Systems Approach to the Large Scale Ocean Circulation and El Niño* (Springer Science, 2005).
- <sup>32</sup>A. Clarke, *An Introduction to the Dynamics of El Niño and the Southern Oscillation* (Academic, London, 2008).
- <sup>33</sup>E. Sarachik and M. Cane, *The El Niño-Southern Oscillation Phenomenon* (Cambridge University Press, 2010).
- <sup>34</sup>C. Wang *et al.*, *El Niño and Southern Oscillation (ENSO): A Review, Coral Reefs of the Eastern Pacific* (Springer, Berlin, 2012), pp. 3–19.
- <sup>35</sup>M. S. Halpern and C. F. Ropelewski, *J. Clim.* **5**, 577 (1992).
- <sup>36</sup>D. Stauffer and A. Aharony, *Introduction to Percolation Theory* (Taylor & Francis, London, 1994).
- <sup>37</sup>A. Bunde and S. Havlin, *Fractals and Disordered Systems* (Springer Science & Business Media, 2012).
- <sup>38</sup>D. P. Dee, *Q. J. R. Meteorol. Soc.* **137**, 553 (2011).
- <sup>39</sup>E. Kalnay *et al.*, *Bull. Am. Meteorol. Soc.* **77**, 437 (1996).
- <sup>40</sup>K. Onogi *et al.*, *J. Met. Soc. Jpn.* **85**, 369 (2007).
- <sup>41</sup>J. Nagler, A. Levina, and M. Timme, *Nat. Phys.* **7**(3), 265–270 (2011).
- <sup>42</sup>J. Fan and X. Chen, *Europhys. Lett.* **107**(2), 28005 (2014).
- <sup>43</sup>B. Bollobás, *Random Graphs* (Cambridge University Press, 2001).
- <sup>44</sup>S. Buldyrev, R. Parshani, G. Paul, H. E. Stanley, and S. Havlin, *Nature* **464**, 1025–1028 (2010).
- <sup>45</sup>D. Achlioptas, R. D’Souza, and J. Spencer, *Science* **323**, 1453–1455 (2009).
- <sup>46</sup>R. A. Costa, S. N. Dorogovtsev, A. V. Goltsev, and J. F. F. Mendes, *Phys. Rev. Lett.* **105**, 255701 (2010).
- <sup>47</sup>O. Riordan and L. Warnke, *Science* **333**, 322 (2011).
- <sup>48</sup>F. Radicchi and S. Fortunato, *Phys. Rev. E* **81**, 036110 (2010).
- <sup>49</sup>P. Grassberger, C. Christensen, G. Bizhani, S. Son, and M. Paczuski, *Phys. Rev. Lett.* **106**, 225701 (2011).
- <sup>50</sup>N. A. M. Araújo, J. S. Andrade, Jr., R. M. Ziff, and H. J. Herrmann, *Phys. Rev. Lett.* **106**, 095703 (2011).
- <sup>51</sup>W. Chen and R. D’Souza, *Phys. Rev. Lett.* **106**, 115701 (2011).
- <sup>52</sup>J. Nagler, T. Tiessen, and H. W. Gutch, *Phys. Rev. X* **2**, 031009 (2012).
- <sup>53</sup>J. Fan, M. Liu, L. Li, and X. Chen, *Phys. Rev. E* **85**, 061110 (2012).
- <sup>54</sup>A. A. Saberi, *Phys. Rev. Lett.* **110**, 178501 (2013).
- <sup>55</sup>V. Rodriguez-Mendez, V. M. Eguiluz, E. H. Garcia, and J. J. Ramasco, *Sci. Rep.* **6**, 29552 (2016).